

The Thermal Diffusivity of the Refrigerants R32, R143a and R125¹

M. Pitschmann² and J. Straub^{2,3}

¹ Paper presented at the Fourteenth Symposium on Thermophysical Properties,
June 25-30, Boulder, Colorado, U.S.A.

² Lehrstuhl A für Thermodynamik, Technische Universität München
Boltzmannstrasse 15, D-85747 Garching, Germany.

³ To whom correspondence should be addressed.

ABSTRACT

The thermal diffusivity of the halogenated fluorocarbons R32, R125 and R143a is systematically measured in a wide region of state around the liquid-vapor critical point using dynamic light scattering as the measuring method. The experimental setup is capable of measuring in homodyne (high light intensity) or heterodyne mode (low light intensity). Especially in the vicinity of the critical point this method is superior to other techniques since no calibration is necessary and the fluid is held in thermodynamic equilibrium. With high light scattering intensities in the near critical region the uncertainty of the measurements is about 0.5% and increases to up to 5% far from the critical state. Measurements were performed in both coexisting phases, along the critical isochore and along seven isotherms. The range of application is characterized in terms of the reduced density and pressure by $0.3 < r / r_c < 2$ and $0.5 < p / p_c < 2.5$. These restrictions are defined by low scattering intensities and by the mechanical limits of the apparatus due to high pressures of the fluid. The corresponding temperature range is from 300 K to 390 K. When approaching the critical point the thermal diffusivity drops by orders of magnitude and can be expressed by simple scaling laws depending on the reduced temperature difference $t = (T - T_c) / T_c$. In addition to the thermal diffusivity the refractive index and the critical parameters T_c , p_c are measured and presented. The density of the fluid is calculated from the refractive index using the Lorentz-Lorenz relation.

KEY WORDS: critical region; light scattering; refrigerants; R32; R125; R143a; thermal diffusivity; transport properties

INTRODUCTION

In search for environmentally acceptable refrigerants the HFC's R32, R125, and R143a show great promise and are used preferably as components in mixtures. Some available blends are R404A (R143a/125/134a), R507A (R143a/125), R407A,B,C (R32/125/134a), and R410A(R32/125). Used as substitutes for the CFC's R22 and R502 these fluids seem to be long-term alternatives due to their ozone depletion potential (ODP) of zero. Further specifications which refrigerants must fulfill are inflammability, low toxicity, chemical stability, the possession of favorable thermodynamic properties as well as a low total equivalent warming impact value (TEWI), and a compatibility with lubricant oils.

Dimensionless numbers such as the Nusselt-, Reynolds-, Prandtl-, Grashof- and the Rayleigh-number include transport properties. These dimensionless numbers are needed to calculate the occurring heat transfer when designing system components. Approaching the liquid-vapor critical point the applicability of conventional stationary and transient methods used to determine the thermal diffusivity is limited. Since these methods induce convection and are influenced by the dynamic temperature propagation, also known as piston effect, they are subject to large errors in the critical region. Therefore experimental data is particularly scarce in this region of state. This paper presents measurements of the thermal diffusivity with the goal to reduce this lack of data for the HFC's R32, R125 and R143a.

2. EXPERIMENTS

2.1 Measurement Method

Dynamic Light Scattering is used as measuring method. This noninvasive optical method is suitable to measure the thermal diffusivity of transparent fluids even in the near vicinity of the liquid-vapor critical point. The fluid is held in thermal equilibrium avoiding disturbing convection. By investigating the relaxation behavior of microscopic thermodynamic fluctuations the information on thermal diffusivity is obtained. Due to the

intrinsically absolute nature of the method there is no need for calibration or introducing correction terms.

In this work Dynamic Light Scattering is used in homodyne and heterodyne mode. Both modes differ in the optical arrangement to detect the scattered light. When homodyne mode is applied only the scattered light \vec{I}_s is detected. In regions of states where the light scattering ability of the fluid is very small, a signal enhancement is achieved by superimposing a local oscillator \vec{I}_0 . Yet, heterodyne experiments are more difficult to perform than homodyne experiments.

The theoretical approach of light scattering from hydrodynamic modes results in a time-correlation function $G(t)$ which is in case of pure fluids a sum of two exponential functions.

$$G(t) = (\vec{I}_s + \vec{I}_0)^2 + \vec{I}_s^2 \cdot b_1 \cdot \exp(-2 \cdot t/t_c) + 2 \cdot \vec{I}_s \cdot \vec{I}_0 \cdot b_2 \cdot \exp(-t/t_c) \quad (1)$$

This general expression contains the experimental constants b_1 and b_2 which are functions of the number of coherence areas detected by the optical system. The decay time t_c is defined as

$$t_c = \frac{1}{a \cdot q^2} \quad (2)$$

Since the simultaneous evaluation of two exponential functions is difficult to achieve, a strict distinction between the homodyne ($\vec{I}_s \gg \vec{I}_0$) and the heterodyne mode ($\vec{I}_0 \gg \vec{I}_s$) has to be performed in order to obtain reliable results. For an explicit treatment of Dynamic Light Scattering and its applications we refer to the literature [1-3].

In addition to thermal diffusivity the temperature, the pressure, and the refractive index of the sample fluid is measured. Using the Lorentz-Lorenz [7, 8] equation the density of the fluid is calculated.

2.1 Experimental Apparatus

The experimental apparatus used in our investigation is shown in Fig.1. and has been described in detail in previous publications [4, 5]. One significant modification has been made by adding a polarization preserving optical fiber to the setup. The fiber (16) in combination with the beam splitters (13, 17), the variable attenuator (14), and the fiber coupler system (15) is used to realize the local oscillator while performing heterodyne measurements. As coherent light source an argon-ion laser is used. The laser is equipped with a frequency stabilizing etalon ($\lambda = 514.5 \text{ nm}$) and has a maximum power output of 300 mW.

Before the laser light is focussed into the test cell it passes through a beam expander. The light scattered by the sample fluid is detected by the photomultiplier with a scattering angle between 5-15°. The statistical average behavior of the dissipative temperature fluctuations is analyzed by a digital correlator which evaluates the output signals of the light detector. A nonlinear regression method based on Marquardt [6] is used to fit the 128 output channels of the correlator to the theoretical exponential function. The thermal diffusivity is calculated from the characteristic decay time of the exponential function.

The temperature of the sample fluid is controlled by 18 platinum resistance thermometers (PT 100) and 8 heater foils. The test cell is capable of providing a long term temperature stability of $\pm 2 \text{ mK}$ over a time period of 24 hours and can reach a temperature of 450 K.

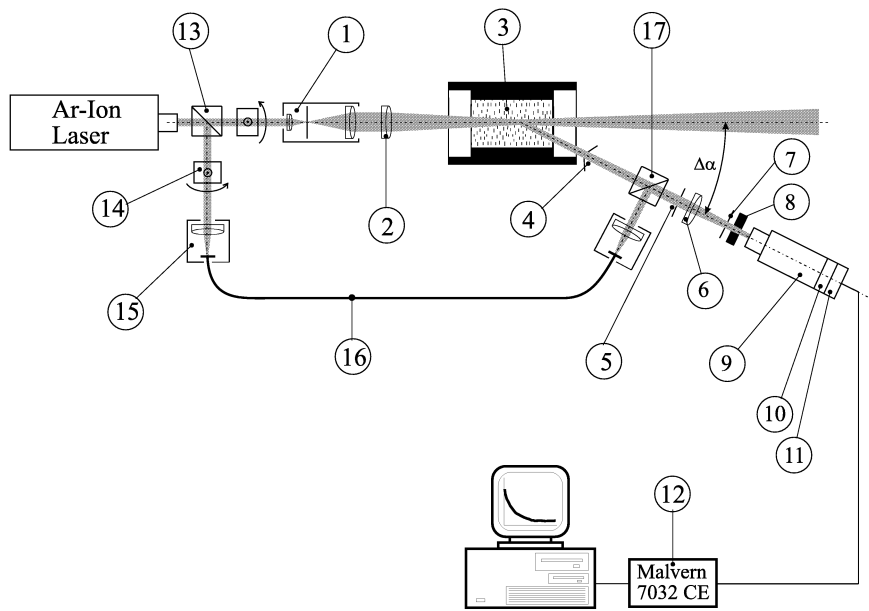


Fig. 1. Experimental apparatus.

Homodyne setup: (1) beam expander; (2) focal lens; (3) sample cell; (4) pinhole; (5) aperture; (6) focal lens; (7) pinhole; (8) interference filter; (9) photomultiplier; (10) preamplifier; (11) discriminator; (12) digital correlator. **Heterodyne extension:** (13) beam splitter; (14) variable attenuator; (15) fiber coupler; (16) polarization preserving fiber, (17) beam splitter

2.2 Accuracies

T, p, r -Data

T: A low-drift platinum resistance thermometer (PT100) with a precision better than 1 mK is used to measure the fluid temperature. The thermometer was calibrated with a standard platinum resistance thermometer (PT25) model 162D which was produced by Rosemount Aerospace Inc. and calibrated by NIST according to the International Temperature Scale of 1990 (ITS-90). The measurement of the critical temperature of R32 was repeated within 2 years, in order to estimate the time dependent temperature drift of the thermometer. The reproducibility was within ± 4 mK. This result also confirms that the filling procedure has no noticeable impact on the purity of the sample fluid. The temperature is estimated to be ± 10 mK.

P: The fluid pressure is measured by a piezo-resistive pressure transducer model 4045A200 which was produced by Kistler Instrumente AG. The precision of the pressure sensor is better than 100 Pa. An oil pressure scale of Dreyer, Rosenkranz & Droop AG. was used to calibrate the pressure sensor. To detect hysteresis effects calibration was performed with increasing and decreasing pressure values. Due to the large pressure range from 0.1-12 MPa the pressure uncertainty is ± 0.01 MPa.

r: Using the Lorentz-Lorenz relation the density is calculated from the refractive index data. The major part of the density uncertainty is caused by the uncertainty of the angle determination when measuring the refractive index. The uncertainty of the high precision dividing head of $\Delta\Theta = 6''$ results in an accuracy of the refractive index of $\Delta n < 5 \cdot 10^{-4}$. Assuming the validity of the Lorentz-Lorenz relation in the whole investigated region of state the density uncertainty better than $\pm 3\%$.

Thermal Diffusivity

The thermal diffusivity is calculated from the decay time t_c and the scattering vector \vec{q} by equation (1)

$$a = \frac{1}{t_c \cdot q^2} \quad (1)$$

The scattering vector \vec{q} defines the scattering geometry and is expressed as

$$|\vec{q}| = q = \frac{4 \cdot \mathbf{p} \cdot \mathbf{n}}{\mathbf{l}_L} \cdot \sin\left(\frac{\Theta}{2}\right) \quad (2)$$

with n as the refractive index of the fluid, \mathbf{l}_L as the wavelength of the laser light and Θ as the scattering angle. While the error of the scattering vector \vec{q} can be calculated easily, the uncertainty of the decay time can be assessed hardly. This is due to the statistical nature of the

measurement method which is reflected in the decay time. A brief estimation of the individual errors and their influence on a is given:

- I_L : The frequency stabilizing etalon reduces the error $\Delta a/a$ due to wavelength fluctuations to the order of 0.001%. Therefore it can be neglected.
- Θ : Since the scattering angle has a strong influence on a it has to be adjusted precisely. The accuracy $\Delta\Theta$ of the high precision dividing head is better than $6''$. This results in an error $\Delta a/a < 0.05\%$.
- n : The used experimental setup allows the determination of the refractive index with an accuracy Δn better than $5 \cdot 10^{-4}$. The influence on a is $\Delta a/a < 0.08\%$.
- t_c : A detailed treatment of the accuracy of light scattering experiments in connection with its statistical nature is given in Ref. [9-11]. Errors caused by afterpulsing and dead-time effects of the detection system or bias are also treated. Further, recommendations for optimizing experimental parameter such as the run time, the count per sample time ratio or the sample time per decay time are given in the references. Other sources of error are gravity, multiple scattering, limits imposed by the hydrodynamic theory and laser heating. These errors are treated in Ref. [5]. If the aforementioned assumptions for the heterodyne ($\vec{I}_0 \gg \vec{I}_s$) and the homodyne mode ($\vec{I}_s \gg \vec{I}_0$) are not satisfied an additional error arises. In homodyne experiments this source of error becomes noticeable further away from the critical point. In this region the contribution of \vec{I}_0 increases due to low light-scattering signals and the corresponding high laser power. The uncertainty of the thermal diffusivity measurements can be calculated hardly. Therefore, each measurement point is averaged from six single measurements, which are performed at different angles. Depending on the region of state, the accuracy of the thermal diffusivity measurements is estimated to 0.5% in the critical region and increases up to 5% in the extended critical region.

3. EXPERIMENTAL RESULTS

Measurements were performed along the critical isochore, both coexisting phases and along four super- and three subcritical isotherms. A systematic coverage of a broad region of state is the objective of this work. In terms of the temperature, the pressure, and the density the covered region of state is approximately $0.1 \text{ MPa} < p < 10 \text{ MPa}$, $300 \text{ K} < T < 390 \text{ K}$ and $100 \text{ kg/m}^3 < \rho < 1200 \text{ kg/m}^3$. The boundaries of the covered region were set by the applicability of the measuring method (limit of low light scattering intensities) and of the apparatus (pressure resistance of the sapphire cell windows). Isothermal measurements were carried out at $t = \pm 10^{-3}$, $\pm 10^{-2}$, $\pm 5 \cdot 10^{-2}$, and $+10^{-1}$, with t denoting the reduced temperature difference $t = (T - T_c)/T_c$. The measurement results are given in the Tables VI, VII, and VIII of the appendix. All fluid samples were supplied by Solvay Fluor und Derivate GmbH with a purity better than 99.9 wt-%.

3.1. Critical Values

Applying an optical method, the critical temperature T_c and the critical pressure p_c are determined. The fluid is heated to a supercritical temperature and after the density relaxation is finished it is cooled down with a temperature ramp of -20 mK/h . With the appearance of the liquid-vapor meniscus the critical temperature and pressure are determined. In Table I the measured critical parameters T_c , p_c , and n_c for all sample fluids are given. The critical density is determined by averaging the literature data listed in the Tables II, III, IV.

Table I. Measured critical parameters (T_c , p_c , n_c) of R32, R125, and R143a

	T_c (ITS-90) (K)	p_c (kPa)	ρ_c ($\text{kg} \cdot \text{m}^{-3}$)	n_c	$LL_c \cdot 10^6$ ($\text{m}^3 \cdot \text{mol}^{-1}$)
R32	351.25 ± 0.01	5743 ± 10	(425)	1.0834	6.701
R125	339.13 ± 0.01	3603 ± 10	(569)	1.0855	11.825
R143a	345.88 ± 0.01	3746 ± 10	(436)	1.0895	11.314

All temperatures refer to or were converted to the ITS-90 temperature scale. For R32 and R125 the T_c values taken from literature vary with a temperature spread of $\Delta T_c \approx 0.3$ K. Even larger is the temperature spread for R143a with $\Delta T_c \approx 0.5$ K. These deviations are probably caused by different purities of the sample fluid and by different measurement methods. Comparing the critical temperature of this work with those taken from literature, good agreement is found for R32. In case of R125 and R143a the critical temperatures are lower than most literature values. All critical pressures determined in this work are lower than the values taken from literature by a difference of up to 40 kPa.

The value of n_c is determined from the refractive index data and in addition with the critical density the Lorentz-Lorenz constant LL_c is calculated. These values are also listed in Table I. The Lorentz-Lorenz constant is used to calculate the density from the appropriate refractive index.

Table II. Critical parameters of R32 taken from literature

T_c (ITS-90) (K)	p_c (kPa)	ρ_c (kg · m ⁻³)	year	author	ref.
351.54±0.2	5830± 6	429.6± 1.2	1968	Malbrunot et al.	[12]
351.26±0.03	5778± 3	425 ± 5	1993	M. Fukushima	[13]
351.26±0.01	5785± 9	427 ± 5	1994	Y. Higashi	[13]
351.36±0.02	-	419 ± 7	1994	J.W. Schmidt et al.	[14]
351.26±0.01	5784	424 ± 1	1995	S. Kuwabara et al.	[15]
351.23±0.06	5783± 6	420 ± 8	1995	M. Nagel et al.	[16]
351.26	5782	424	1996	NIST	[17]
351.23	5783	419.8	1996	Solvay Fluor & Derivate Inc.	[18]
351.25± 0.01	5743 ± 10	-	1999	this work	

Table III. Critical parameters of R125 taken from literature

T_c (ITS-90) (K)	p_c (kPa)	ρ_c (kg · m ⁻³)	year	author	ref.
339.17 ± 0.2	3595 ± 10	571.3 ± 3	1992	L. C. Wilson et al.	[19]
339.18 ± 0.03	3621 ± 3	562 ± 5	1992	M. Fukushima et al.	[20]
339.17 ± 0.01	3620 ± 6	577 ± 5	1994	Y. Higashi	[13]
339.33 ± 0.02	-	565 ± 9	1994	J.W. Schmidt et al.	[14]
339.165 ± 0.01	-	568 ± 1	1995	S. Kuwabara et al.	[15]
339.43 ± 0.06	3635 ± 6	211.4 ± 8	1995	M. Nagel et al.	[16]
339.33	3629	571.3	1996	NIST	[17]
339.43	3635	567.9	1996	Solvay Fluor & Derivate Inc.	[18]
339.13 ± 0.01	3603 ± 10	-	1999	this work	

Table IV. Critical parameters of R143a taken from literature

T_c (ITS-90) (K)	p_c (kPa)	ρ_c (kg · m ⁻³)	year	author	ref.
346.23 ± 0.5	3757 ± 70	434 ± 10	1955	W.H. Mears	[21]
346 ± 0.1	3787 ± 15	455 ± 5	1991	Arnaud et al.	[22]
345.97 ± 0.03	3769 ± 5	429 ± 3	1993	M. Fukushima	[23]
346.18 ± 0.05	3780 ± 6	442 ± 4	1993	Wang et al.	[24]
345.88 ± 0.01	3764 ± 5	431 ± 3	1996	Y. Higashi et al.	[25]
346.04 ± 0.02	-	-	1996	J.W. Schmidt et al.	[26]
345.75 ± 0.06	3765 ± 6	427 ± 9	1996	M. Nagel & K. Bier	[27]
346.04	3776	432.9	1996	NIST	[17]
346	3785	425.7	1996	Solvay Fluor & Derivate Inc.	[18]
345.88 ± 0.01	3746 ± 10	-	1999	this work	

3.2. Thermal Diffusivity

A simple power law is used to describe the thermal diffusivity data obtained along the critical isochore. In accordance with scaling theory the thermal diffusivity data is fitted to the expression:

$$a = a_0 \cdot t^m \quad (3)$$

For the critical isochore the thermal diffusivity data is accurately expressed by this equation in the entire investigated range. Measurements performed in the 2-phase region exclusively obey Eq. (3) in the near vicinity of the critical point. Thus, an additional temperature dependent

term is added to the exponent to consider deviations when the distance to the critical point is increased. The data of the vapor- and liquid phase is expressed by the equation

$$a = a_0 \cdot |t|^{(m_0 + m_1 |t|)} \quad (4)$$

The coefficients listed in Table V. are obtained by regression analyses applying Eqs. (3) and (4). The exponent m of Eq. (3) ranges in between $0.77 < m < 0.84$ for all sample fluids. In case of the vapor and liquid phase the coefficient m_0 varies between $0.758 < m_0 < 1.162$. In all cases the exponents are larger than the theoretical value $n = 0.63$ deduced by the scaling theory. An explanation for the discrepancy between the measured and the theoretical exponent is given by Sengers et al. [28] exemplary for the thermal conductivity. The fluid property has to be split into two terms. One describing the critical enhancement and one considering the background which is calculated by extrapolating the behavior of the non-critical data into the critical region. Yet, it is difficult to determine an expression for the background term as well as for the thermal diffusivity data obtained along the isotherms. The behavior of the thermal diffusivity is shown in Fig. 2, 3 with R125 serving as exemplary fluid.

Table V. Coefficients in Eqs. (3) and (4)

	<u>critical isochore</u>		<u>liquid phase</u>			<u>vapor phase</u>		
	$a_0 \cdot 10^7$ (m^2/s)	μ	$a_0 \cdot 10^7$ (m^2/s)	μ_0	μ_1	$a_0 \cdot 10^7$ (m^2/s)	μ_0	μ_1
R32	2.359	0.815	9.407	0.869	3.526	4.272	0.758	-1.481
R125	1.724	0.776	5.021	0.784	3.843	16.680	0.993	2.314
R143a	2.581	0.836	10.716	0.904	5.561	42.666	1.162	3.452

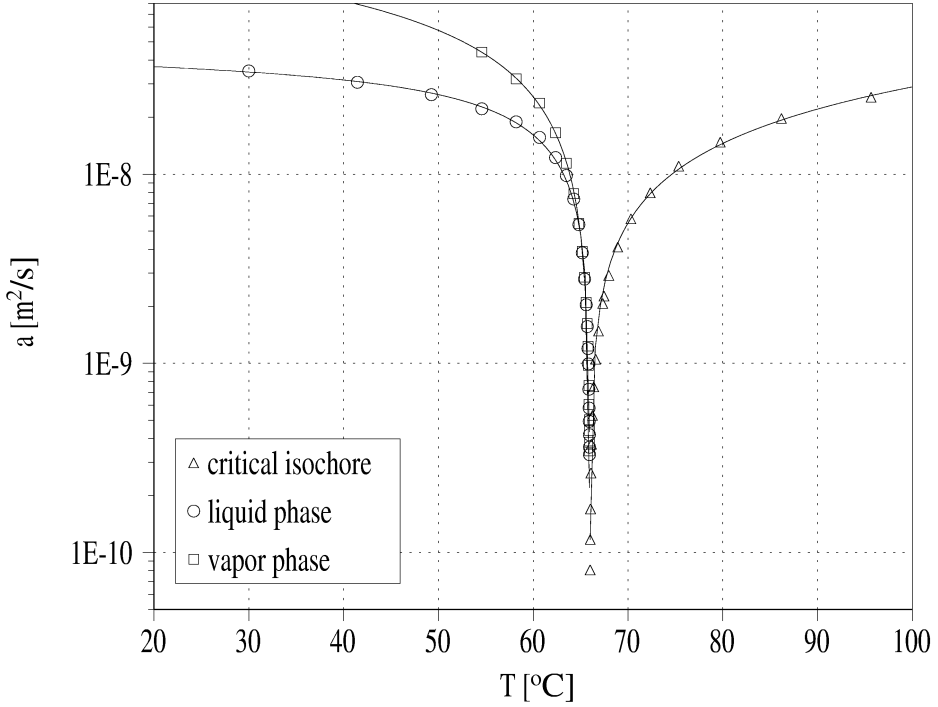


Fig. 2. The thermal diffusivity of R125 plotted versus the temperature.

Measurements were obtained along the critical isochore and in both coexisting phases.

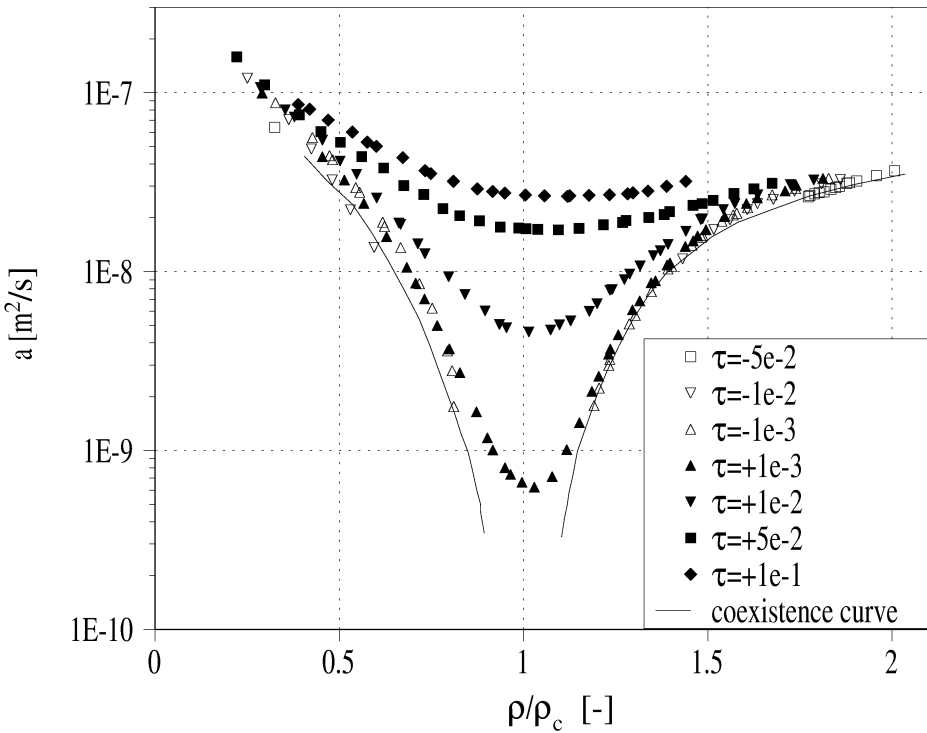


Fig. 3. The thermal diffusivity of R125 plotted versus the reduced density ρ / ρ_c .

4. CONCLUSIONS

The results of thermal diffusivity measurements have been presented, using R32, R125, and R143a as sample fluids. As measuring method dynamic light scattering was used, permitting accurate measurements even in the vicinity of the liquid-vapor critical point. In terms of the density the investigated region is $100 \text{ kg} \cdot \text{m}^{-3} < r < 1200 \text{ kg} \cdot \text{m}^{-3}$. The accuracy of the measurements is estimated to be better than 5%. Since the thermal diffusivity values cover a range of four orders of magnitude, it is difficult to establish a comprehensive equation which describes all of the measurement data. The measurements obtained along the critical isochore and in both coexisting phases can be described by power laws within 10%.

ACKNOWLEDGMENTS

The authors would like to express their gratitude to the Deutsche Forschungsgemeinschaft (DFG) for supporting this research project. Further, the authors are grateful to Solvay Fluor und Derivate GmbH for the supply of the fluid samples.

REFERENCES

- [1] B. Chu, *Laser Light Scattering*, Academic Press, New York, 1974
- [2] B. J. Berne and R. Pecora, *Dynamic Light Scattering*, Wiley, New York, 1976
- [3] R. Pecora, *Dynamic Light Scattering; Applications of Photon Correlation Spectroscopy*, Plenum Press, New York, 1985
- [4] B. Kruppa and J. Straub, *Exp. Therm. Fluid Sci.*, 6 (1993) 28-38
- [5] B. Kruppa, P. Jany, and J. Straub, *Int. J. Thermophys.*, 9 (1988) 911-921
- [6] J. Ahrendts and H.D. Baehr, *Forschung Ingenieur Wesen*, 45 (1979) 51-56
- [7] H. A. Lorentz, *Ann. der Physik und Chemie*, 9 (1880) 641-665
- [8] L. Lorenz, *Ann. der Physik und Chemie*, 11 (1880) 70-103

- [9] B. Kruppa, Die Temperaturleitfähigkeit alternativer Kältemittel in einem weiten Temperatur- und Dichtebereich, PH. D. Thesis, Technische Universität München, 1993
- [10] E. Jakeman, E. R. Pike, and S. Swain, J. Phys. A, 4 (1971), 517-534
- [11] V. Degiorgio and L. B. Lastovka, Phys. Rev. A, 4 (1971), 2033
- [12] P. F. Malbrunnot et al., J. Chem. Eng. Data, 13 (1968), 16-20
- [13] Y. Higashi, Int. J. Refrig., 17 (1994), 524-531
- [14] J. W. Schmidt and M. R. Moldover, J. Chem. Eng. Data, 39 (1994), 39-44
- [15] S. Kuwabara et al., J. Chem. Eng. Data, 40 (1995), 112-116
- [16] M. Nagel and K. Bier, Int. J. Refrig., 18 (1995), 534-543
- [17] M. O. McLinden et al., NIST Standard Reference Database 23, Version 6.0 (1998)
- [18] Solvay Fluor und Derivate GmbH, Refrigerant Software, Version 1.0 (1996)
- [19] L.C. Wilson et al., Fluid Phase Equilibria, 80 (1992), 167-177
- [20] M. Fukushima and S. Ohtoshi, Proc. of the 13th Japan Symposium on Thermophysical Properties, Akita, (1992), 49-52
- [21] W. H. Mears et al., Industrial and engineering chemistry, 47 (1955), 1449-1454
- [22] D. Arnaud et al., 18th Int. Congress Refrigeration, Montreal, (1991), 664-668
- [23] M. Fukushima, Trans. JAR, 10 (1993), 87-93
- [24] H. Wang et al., Beijing Gongcheng Rewuli Xuebao, 14 (1993), 122-124
- [25] Y. Higashi and T. Ikeda, Fluid Phase Equilibria, 125 (1996), 139-147
- [26] W. Schmidt et al., Fluid Phase Equilibria, 122 (1996), 187-206
- [27] M. Nagel and K. Bier, Int. J. Refrig., 19 (1996), 264-271
- [28] J. V. Sengers, P. H. Keyes, Phys. Rev. Lett., 26 (1971), 70-73

APPENDIX: Experimental results for R32, R125, and R143a

Table VI. Experimental results for R32 / critical isochore

T (K)	P (MPa)	n	ρ (kg · m ⁻³)	$a \cdot 10^9$ (m ² · s ⁻¹)
351.27	5.75	1.0834	425.3	0.087
351.29	5.75	1.0834	425.3	0.146
351.32	5.75	1.0834	425.3	0.226
351.34	5.76	1.0834	425.3	0.306
351.40	5.76	1.0834	425.3	0.433
351.47	5.77	1.0834	425.3	0.583
351.59	5.78	1.0834	425.3	0.791
351.75	5.80	1.0834	425.3	1.066
352.00	5.83	1.0834	425.3	1.474
352.33	5.88	1.0834	425.3	2.004
352.77	5.93	1.0834	425.3	2.661
353.64	6.04	1.0834	425.3	3.917
354.77	6.18	1.0834	425.3	5.388
356.42	6.39	1.0834	425.3	7.470
358.83	6.69	1.0834	425.3	10.410
362.41	7.15	1.0834	425.3	14.534
367.65	7.82	1.0834	425.3	19.572
375.32	8.82	1.0834	425.3	26.254

Table VI (continued). Experimental results for R32 / 2 phase region

T (K)	P (MPa)	n_l	n_v	ρ_l (kg · m ⁻³)	ρ_v (kg · m ⁻³)	$a_l \cdot 10^9$ (m ² · s ⁻¹)	$a_v \cdot 10^9$ (m ² · s ⁻¹)
318.47	2.80	1.1737	1.0157	867.8	81.2	55.030	98.445
328.91	3.56	1.1605	1.0220	804.4	113.5	46.289	68.954
336.02	4.16	1.1500	1.0284	753.6	146.3	37.484	47.106
340.87	4.62	1.1407	1.0345	708.3	177.6	30.271	35.053
344.17	4.96	1.1331	1.0399	671.1	204.9	24.321	25.459
346.42	5.19	1.1266	1.0448	639.2	230.2	19.045	18.805
347.95	5.36	1.1212	1.0492	612.5	252.4	14.195	13.331
348.99	5.48	1.1162	1.0531	588.1	272.4	10.330	9.752
349.69	5.56	1.1119	1.0569	567.0	291.3	7.589	7.094
350.20	5.62	1.1083	1.0597	549.0	305.6	5.465	5.186
350.52	5.66	1.1054	1.0624	534.9	319.3	4.053	3.818
350.73	5.68	1.1027	1.0647	521.5	331.1	2.967	2.947
350.91	5.70	1.1004	1.0667	509.7	341.2	2.103	2.165
351.01	5.71	1.0984	1.0684	499.7	349.8	1.536	1.499
351.08	5.72	1.0969	1.0699	492.6	357.0	1.093	1.126
351.13	5.73	1.0951	1.0711	483.6	363.2	0.805	0.888
351.16	5.73	1.0942	1.0721	478.9	368.3	0.621	0.687
351.19	5.74	1.0932	1.0731	473.9	373.3	0.469	0.517
351.20	5.74	1.0925	1.0740	470.7	377.9	0.356	0.408
351.21	5.74	1.0921	1.0744	468.6	379.7	0.297	0.331
351.218	5.74	1.0918	1.0752	466.8	384.0	0.241	0.283
351.223	5.74	1.0912	1.0755	463.9	385.3	0.203	0.248

Table VI (continued). Experimental results for R32 / isotherm $t = -5e^{-2}$

T (K)	P (MPa)	n	ρ (kg · m ⁻³)	$a \cdot 10^9$ (m ² · s ⁻¹)
333.69	5.68	1.1618	810.5	50.236
333.69	5.14	1.1597	800.6	47.750
333.69	4.52	1.1568	786.6	44.280
333.69	4.25	1.1557	781.0	43.222
333.69	3.99	1.1544	774.7	41.217
333.69	3.96	1.1539	772.6	40.949
333.69	3.96	1.0262	135.0	53.947
333.69	3.61	1.0214	110.4	78.943
333.69	3.34	1.0187	96.2	97.632

Table VI (continued). Experimental results for R32 / isotherm $t = -1e^{-2}$

T (K)	P (MPa)	n	ρ (kg · m ⁻³)	$a \cdot 10^9$ (m ² · s ⁻¹)
347.74	9.38	1.1558	781.5	50.394
347.74	8.81	1.1529	767.7	48.609
347.74	8.20	1.1506	756.2	45.861
347.74	6.93	1.1436	722.5	38.476
347.74	6.69	1.1418	713.7	36.177
347.74	6.52	1.1403	706.3	35.017
347.74	6.44	1.1397	703.5	34.363
347.74	6.29	1.1385	697.6	33.031
347.74	6.10	1.1364	687.5	31.262
347.74	5.82	1.1330	670.5	26.956
347.74	5.59	1.1292	652.2	22.082
347.74	5.33	1.1216	614.9	14.534
347.74	5.33	1.0484	248.3	13.829
347.74	5.28	1.0438	224.7	21.734
347.74	5.17	1.0401	205.9	30.223
347.74	5.01	1.0354	182.3	42.365
347.74	4.64	1.0293	150.7	64.532
347.74	4.35	1.0253	130.2	87.891

Table VI (continued). Experimental results for R32 / isotherm $t = -1e^{-3}$

T (K)	P (MPa)	n	ρ (kg · m ⁻³)	$a \cdot 10^9$ (m ² · s ⁻¹)
350.90	8.60	1.1474	740.8	46.208
350.90	8.11	1.1444	726.5	42.342
350.90	7.51	1.1407	708.5	38.227
350.90	7.00	1.1367	689.0	34.935
350.90	6.54	1.1337	674.3	31.404
350.90	6.51	1.1315	663.4	28.109
350.90	6.22	1.1289	650.8	24.115
350.90	6.07	1.1245	628.8	18.882
350.90	5.99	1.1235	623.8	17.838
350.90	5.97	1.1223	618.1	16.359
350.90	5.95	1.1210	611.9	15.261

T (K)	P (MPa)	n	ρ (kg · m ⁻³)	$a \cdot 10^9$ (m ² · s ⁻¹)
350.90	5.89	1.1190	602.0	13.504
350.90	5.85	1.1187	600.2	13.006
350.90	5.76	1.1124	569.4	8.510
350.90	5.71	1.1067	540.9	5.032
350.90	5.71	1.1039	527.0	3.760
350.90	5.71	1.1025	520.5	3.107
350.90	5.71	1.1006	510.7	2.243
350.90	5.71	1.0675	345.0	2.097
350.90	5.70	1.0664	339.4	2.639
350.90	5.69	1.0637	326.0	3.800
350.90	5.69	1.0616	315.5	4.974
350.90	5.68	1.0604	309.1	5.728
350.90	5.68	1.0601	307.5	5.906
350.90	5.68	1.0585	299.7	7.347
350.90	5.65	1.0569	291.3	9.150
350.90	5.64	1.0529	271.4	12.825
350.90	5.63	1.0527	270.1	13.067
350.90	5.60	1.0503	257.9	15.690
350.90	5.54	1.0490	251.5	17.533
350.90	5.45	1.0450	231.2	22.968
350.90	5.24	1.0391	201.1	35.797
350.90	4.94	1.0334	172.1	48.860

Table VI (continued). Experimental results for R32 / isotherm $t = +1e^{-3}$

T (K)	P (MPa)	n	ρ (kg · m ⁻³)	$a \cdot 10^9$ (m ² · s ⁻¹)
351.60	8.75	1.1471	739.3	45.050
351.60	8.07	1.1432	720.3	41.058
351.60	7.54	1.1395	702.6	37.765
351.60	7.02	1.1353	681.8	33.654
351.60	6.59	1.1323	667.3	30.499
351.60	6.40	1.1295	653.4	27.188
351.60	6.25	1.1265	638.9	24.442
351.60	6.14	1.1241	627.2	22.294
351.60	6.10	1.1224	618.4	19.292
351.60	5.99	1.1175	594.5	14.840
351.60	5.95	1.1169	591.4	14.172
351.60	5.92	1.1143	578.9	11.432
351.60	5.85	1.1099	557.2	7.896
351.60	5.85	1.1097	556.1	7.612
351.60	5.84	1.1071	543.1	6.037
351.60	5.84	1.1064	539.7	5.553
351.60	5.81	1.1032	523.9	4.044
351.60	5.81	1.1005	510.5	2.824
351.60	5.80	1.0968	491.8	1.828
351.60	5.79	1.0938	476.8	1.282
351.60	5.79	1.0917	466.5	0.991
351.60	5.79	1.0904	459.9	0.904

T (K)	P (MPa)	n	ρ (kg · m ⁻³)	$a \cdot 10^9$ (m ² · s ⁻¹)
351.60	5.79	1.0893	454.4	0.827
351.60	5.79	1.0874	444.8	0.772
351.60	5.79	1.0835	425.5	0.767
351.60	5.78	1.0818	417.0	0.843
351.60	5.78	1.0806	411.1	0.978
351.60	5.78	1.0780	397.8	1.268
351.60	5.78	1.0752	384.0	1.726
351.60	5.78	1.0731	373.1	2.261
351.60	5.78	1.0716	365.9	2.526
351.60	5.78	1.0695	355.2	3.191
351.60	5.77	1.0661	337.8	4.245
351.60	5.76	1.0621	317.7	6.132
351.60	5.74	1.0593	303.5	7.901
351.60	5.73	1.0573	293.5	9.693
351.60	5.69	1.0554	283.8	11.569
351.60	5.59	1.0491	252.0	19.153
351.60	5.58	1.0476	244.5	20.975
351.60	5.43	1.0431	221.5	28.905
351.60	5.26	1.0386	198.2	39.589
351.60	5.08	1.0355	182.7	48.166
351.60	4.63	1.0286	147.1	73.042
351.60	3.22	1.0162	83.7	147.894

Table VI (continued). Experimental results for R32 / isotherm $t = +1e^{-2}$

T (K)	P (MPa)	n	ρ (kg · m ⁻³)	$a \cdot 10^9$ (m ² · s ⁻¹)
354.76	8.42	1.1412	710.7	41.403
354.76	7.84	1.1369	689.7	38.367
354.76	7.48	1.1336	673.4	35.028
354.76	7.16	1.1297	654.3	31.136
354.76	6.62	1.1196	605.1	21.057
354.76	6.41	1.1121	568.1	14.119
354.76	6.34	1.1078	546.4	11.473
354.76	6.28	1.1022	518.6	8.512
354.76	6.25	1.0996	505.9	7.712
354.76	6.23	1.0955	485.4	6.567
354.76	6.21	1.0917	466.7	5.887
354.76	6.19	1.0887	451.6	5.548
354.76	6.18	1.0855	435.5	5.373
354.76	6.16	1.0810	412.9	5.641
354.76	6.14	1.0773	394.3	6.170
354.76	6.13	1.0743	379.4	6.798
354.76	6.10	1.0700	357.7	8.214
354.76	6.07	1.0656	335.3	10.312
354.76	6.03	1.0618	316.5	13.589
354.76	5.97	1.0571	292.6	16.621
354.76	5.88	1.0520	266.8	21.925
354.76	5.77	1.0478	245.5	29.570

T (K)	P (MPa)	n	ρ (kg · m ⁻³)	$a \cdot 10^9$ (m ² · s ⁻¹)
354.76	5.67	1.0447	229.5	34.206
354.76	5.53	1.0409	210.3	41.514
354.76	5.34	1.0375	192.7	49.692
354.76	3.94	1.0208	107.3	121.530

Table VI (continued). Experimental results for R32 / isotherm $t = +5e^{-2}$

T (K)	P (MPa)	n	ρ (kg · m ⁻³)	$a \cdot 10^9$ (m ² · s ⁻¹)
368.81	8.75	1.1075	545.0	28.585
368.81	8.29	1.0967	491.6	21.192
368.81	7.90	1.0835	425.3	19.182
368.81	7.68	1.0751	383.5	21.017
368.81	7.48	1.0683	349.1	22.933
368.81	7.37	1.0643	329.0	24.655
368.81	7.22	1.0599	306.8	27.524
368.81	7.03	1.0551	282.3	33.294
368.81	6.73	1.0486	249.4	42.770
368.81	6.45	1.0436	224.0	51.814
368.81	5.96	1.0366	188.2	69.573

Table VI (continued). Experimental results for R32 / isotherm $t = +1e^{-1}$

T (K)	P (MPa)	n	ρ (kg · m ⁻³)	$a \cdot 10^9$ (m ² · s ⁻¹)
386.37	8.72	1.0608	311.4	44.578
386.37	8.37	1.0555	284.5	48.879
386.37	7.89	1.0490	251.4	56.866
386.37	7.57	1.0450	231.1	65.129
386.37	7.16	1.0405	208.1	75.669
386.37	6.53	1.0349	179.3	90.089
386.37	5.38	1.0254	130.9	131.704

Table VII (continued). Experimental results for R125 / critical isochore

T (K)	P (MPa)	n	ρ (kg · m ⁻³)	$a \cdot 10^9$ (m ² · s ⁻¹)
339.16	3.60	1.0855	569.4	0.081
339.17	3.60	1.0855	569.4	0.117
339.20	3.60	1.0855	569.4	0.170
339.24	3.61	1.0855	569.4	0.263
339.30	3.61	1.0855	569.4	0.374
339.40	3.62	1.0855	569.4	0.530
339.54	3.63	1.0855	569.4	0.750
339.74	3.65	1.0855	569.4	1.050
340.04	3.67	1.0855	569.4	1.480
340.48	3.71	1.0855	569.4	2.072
340.62	3.72	1.0855	569.4	2.267
341.13	3.76	1.0855	569.4	2.917
342.07	3.83	1.0855	569.4	4.113

T (K)	P (MPa)	n	ρ (kg · m ⁻³)	$a \cdot 10^9$ (m ² · s ⁻¹)
343.46	3.95	1.0855	569.4	5.806
345.50	4.11	1.0855	569.4	7.973
348.50	4.36	1.0855	569.4	11.025
352.89	4.72	1.0855	569.4	14.755
359.34	5.25	1.0855	569.4	19.688
368.80	6.04	1.0855	569.4	25.474

Table VII (continued). Experimental results for R125 / 2 phase region

T (K)	P (MPa)	n_l	n_v	ρ_l (kg · m ⁻³)	ρ_v (kg · m ⁻³)	$a_l \cdot 10^9$ (m ² · s ⁻¹)	$a_v \cdot 10^9$ (m ² · s ⁻¹)
303.14	1.57	1.1778		1159.3		35.117	
314.60	2.08	1.1650		1079.0		30.598	
322.41	2.49	1.1539		1009.2		26.314	
327.73	2.81	1.1448	1.0343	952.3	230.6	22.145	44.191
331.35	3.04	1.1368	1.0397	901.2	266.5	18.897	31.912
333.82	3.21	1.1304	1.0454	860.2	305.0	15.632	23.743
335.51	3.33	1.1246	1.0499	822.8	334.5	12.230	16.533
336.65	3.41	1.1195	1.0538	790.3	360.6	9.833	11.422
337.43	3.47	1.1152	1.0575	762.4	384.9	7.384	7.877
337.97	3.51	1.1115	1.0609	738.5	407.5	5.409	5.483
338.33	3.54	1.1081	1.0634	716.7	424.0	3.837	3.902
338.57	3.56	1.1053	1.0655	698.5	437.6	2.787	2.852
338.74	3.57	1.1029	1.0675	682.8	451.0	2.038	2.099
338.86	3.58	1.1012	1.0692	671.8	462.5	1.564	1.621
338.93	3.58	1.0995	1.0708	660.5	473.0	1.196	1.232
338.97	3.59	1.0982	1.0725	652.6	483.8	0.992	0.975
339.02	3.59	1.0972	1.0735	645.7	490.8	0.729	0.763
339.05	3.59	1.0962	1.0744	639.5	496.7	0.580	0.606
339.06	3.59	1.0958	1.0753	636.7	502.6	0.493	0.503
339.08	3.59	1.0952	1.0754	632.6	503.3	0.419	0.442
339.085	3.59	1.0948	1.0759	629.8	506.5	0.360	0.382
339.091	3.60	1.0945	1.0762	628.1	508.6	0.329	0.344

Table VII (continued). Experimental results for R125 / isotherm $t = -5e^{-2}$

T (K)	P (MPa)	n	ρ (kg · m ⁻³)	$a \cdot 10^9$ (m ² · s ⁻¹)
322.18	7.89	1.1751	1142.7	36.603
322.18	6.25	1.1706	1114.5	34.317
322.18	4.75	1.1658	1084.1	32.125
322.18	4.30	1.1640	1073.2	31.357
322.18	4.16	1.1633	1068.9	31.163
322.18	3.77	1.1616	1057.7	29.914
322.18	3.54	1.1606	1051.7	29.450
322.18	3.34	1.1595	1044.4	28.841
322.18	3.04	1.1578	1033.8	27.924
322.18	2.87	1.1566	1026.2	27.598
322.18	2.72	1.1555	1019.2	27.215
322.18	2.58	1.1543	1012.1	26.637
322.18	2.52	1.1539	1009.5	26.174
322.18	2.52	1.0275	184.9	64.047

Table VII (continued). Experimental results for R125 / isotherm $t = -1e^{-2}$

T (K)	P (MPa)	n	ρ (kg · m ⁻³)	$a \cdot 10^9$ (m ² · s ⁻¹)
335.74	7.62	1.1617	1058.9	32.728
335.74	6.53	1.1571	1029.7	30.894
335.74	5.30	1.1505	988.1	28.190
335.74	4.60	1.1454	955.3	25.350
335.74	4.21	1.1415	930.9	23.969
335.74	4.00	1.1391	915.1	22.172
335.74	3.72	1.1348	888.4	19.475
335.74	3.56	1.1310	863.3	17.182
335.74	3.35	1.1234	815.0	11.774
335.74	3.35	1.0505	338.4	13.644
335.74	3.29	1.0449	301.7	22.156
335.74	3.21	1.0407	273.7	32.475
335.74	3.08	1.0359	241.4	48.452
335.74	2.91	1.0307	206.4	70.687
335.74	2.43	1.0212	142.6	120.306

Table VII (continued). Experimental results for R125 / isotherm $t = -1e^{-3}$

T (K)	P (MPa)	n	ρ (kg · m ⁻³)	$a \cdot 10^9$ (m ² · s ⁻¹)
338.79	7.76	1.1589	1040.8	33.224
338.79	6.03	1.1508	989.6	29.134
338.79	5.20	1.1451	953.5	26.826
338.79	4.57	1.1390	915.5	22.802
338.79	4.41	1.1364	898.7	21.199
338.79	4.30	1.1356	893.3	20.732
338.79	4.14	1.1329	875.9	19.084
338.79	3.94	1.1282	846.3	15.930
338.79	3.91	1.1279	844.3	15.575

T (K)	P (MPa)	n	ρ (kg · m ⁻³)	$a \cdot 10^9$ (m ² · s ⁻¹)
338.79	3.83	1.1256	829.4	14.065
338.79	3.73	1.1207	798.2	10.690
338.79	3.71	1.1199	792.4	10.328
338.79	3.63	1.1159	766.9	7.732
338.79	3.62	1.1120	742.0	5.692
338.79	3.61	1.1106	732.8	5.110
338.79	3.59	1.1060	702.7	3.222
338.79	3.59	1.1057	701.0	2.987
338.79	3.59	1.1034	686.2	2.232
338.79	3.58	1.1022	678.3	1.781
338.79	3.58	1.0691	461.4	1.764
338.79	3.58	1.0687	459.0	2.789
338.79	3.58	1.0676	451.7	3.597
338.79	3.57	1.0640	428.2	6.245
338.79	3.55	1.0610	408.2	8.567
338.79	3.53	1.0566	379.4	13.614
338.79	3.52	1.0529	354.4	17.885
338.79	3.51	1.0525	351.6	18.902
338.79	3.47	1.0471	316.0	27.757
338.79	3.44	1.0462	310.0	29.423
338.79	3.36	1.0408	274.2	42.323
338.79	3.31	1.0401	269.3	44.522
338.79	3.21	1.0361	243.0	56.152
338.79	2.85	1.0276	186.0	87.777

Table VII (continued). Experimental results for R32 / isotherm $t = +1e^{-3}$

T (K)	P (MPa)	n	ρ (kg · m ⁻³)	$a \cdot 10^9$ (m ² · s ⁻¹)
339.47	7.57	1.1575	1031.9	33.155
339.47	6.26	1.1510	990.6	30.403
339.47	5.83	1.1483	973.6	28.258
339.47	4.93	1.1414	930.6	25.811
339.47	4.68	1.1388	913.8	24.003
339.47	4.30	1.1335	880.2	20.317
339.47	4.05	1.1290	851.1	17.155
339.47	3.98	1.1270	838.3	15.830
339.47	3.94	1.1259	831.5	14.864
339.47	3.89	1.1240	819.3	13.820
339.47	3.80	1.1203	795.5	11.169
339.47	3.78	1.1196	791.1	10.872
339.47	3.74	1.1168	773.1	8.891
339.47	3.71	1.1158	766.6	8.655
339.47	3.70	1.1131	748.9	6.865
339.47	3.67	1.1114	737.6	6.107
339.47	3.66	1.1080	715.7	4.427
339.47	3.66	1.1061	703.4	3.691
339.47	3.65	1.1057	700.7	3.456
339.47	3.65	1.1033	685.6	2.602

T (K)	P (MPa)	n	ρ (kg · m ⁻³)	$a \cdot 10^9$ (m ² · s ⁻¹)
339.47	3.65	1.1017	674.9	2.138
339.47	3.64	1.0987	655.7	1.431
339.47	3.64	1.0957	636.1	1.012
339.47	3.64	1.0923	613.6	0.715
339.47	3.64	1.0880	586.0	0.624
339.47	3.64	1.0851	566.9	0.664
339.47	3.63	1.0824	549.2	0.734
339.47	3.63	1.0811	540.6	0.801
339.47	3.63	1.0782	521.8	1.005
339.47	3.63	1.0770	513.4	1.178
339.47	3.63	1.0744	496.4	1.645
339.47	3.62	1.0705	470.9	2.720
339.47	3.62	1.0680	454.5	3.703
339.47	3.62	1.0652	435.9	4.999
339.47	3.61	1.0622	416.3	7.028
339.47	3.60	1.0602	402.6	8.619
339.47	3.59	1.0581	388.9	10.579
339.47	3.55	1.0534	357.6	15.687
339.47	3.49	1.0481	322.4	24.086
339.47	3.41	1.0435	292.3	32.538
339.47	3.28	1.0384	258.3	43.919
339.47	2.70	1.0246	165.4	99.569

Table VII (continued). Experimental results for R125 / isotherm $t = +1e^{-2}$

T (K)	P (MPa)	n	ρ (kg · m ⁻³)	$a \cdot 10^9$ (m ² · s ⁻¹)
342.52	7.86	1.1552	1017.8	32.564
342.52	6.74	1.1496	981.8	30.619
342.52	5.56	1.1415	931.2	26.825
342.52	5.00	1.1360	895.9	23.956
342.52	4.78	1.1332	878.0	22.252
342.52	4.49	1.1282	845.9	19.709
342.52	4.48	1.1278	843.2	19.534
342.52	4.30	1.1242	820.2	16.810
342.52	4.18	1.1199	792.7	14.183
342.52	4.14	1.1180	780.8	13.061
342.52	4.07	1.1164	769.9	12.297
342.52	4.02	1.1132	749.4	10.744
342.52	4.00	1.1107	733.4	9.670
342.52	3.99	1.1094	725.2	9.026
342.52	3.96	1.1065	706.3	7.930
342.52	3.95	1.1060	702.9	7.860
342.52	3.95	1.1029	683.0	6.600
342.52	3.93	1.1011	671.0	5.987
342.52	3.91	1.0966	642.1	5.297
342.52	3.90	1.0940	624.9	5.036
342.52	3.89	1.0919	611.1	4.716

T (K)	P (MPa)	n	ρ (kg · m ⁻³)	$a \cdot 10^9$ (m ² · s ⁻¹)
342.52	3.88	1.0867	577.5	4.593
342.52	3.86	1.0814	542.9	4.847
342.52	3.86	1.0798	532.1	5.057
342.52	3.84	1.0764	509.8	6.028
342.52	3.83	1.0717	478.8	7.444
342.52	3.81	1.0679	453.6	9.351
342.52	3.77	1.0623	416.9	12.575
342.52	3.77	1.0607	406.0	14.272
342.52	3.71	1.0566	379.3	18.360
342.52	3.69	1.0562	376.5	18.655
342.52	3.63	1.0511	342.3	25.742
342.52	3.53	1.0464	311.3	35.001
342.52	3.43	1.0426	285.8	41.449
342.52	3.30	1.0385	258.5	54.233
342.52	3.03	1.0320	215.1	73.145
342.52	2.91	1.0299	201.0	80.272
342.52	2.62	1.0242	162.7	107.091

Table VII (continued). Experimental results for R125 / isotherm $t = +5e^{-2}$

T (K)	P (MPa)	n	ρ (kg · m ⁻³)	$a \cdot 10^9$ (m ² · s ⁻¹)
356.09	8.60	1.1450	953.5	31.108
356.09	7.87	1.1406	925.3	28.993
356.09	7.25	1.1357	894.4	27.314
356.09	6.71	1.1307	862.3	24.958
356.09	6.47	1.1281	845.3	24.005
356.09	6.33	1.1259	831.2	23.425
356.09	5.97	1.1202	794.9	21.639
356.09	5.92	1.1190	786.7	20.844
356.09	5.72	1.1153	762.9	20.065
356.09	5.51	1.1098	727.7	19.303
356.09	5.47	1.1090	722.3	18.811
356.09	5.35	1.1044	692.8	18.244
356.09	5.20	1.0986	655.0	17.448
356.09	5.09	1.0938	623.3	17.115
356.09	5.00	1.0888	591.2	17.210
356.09	4.95	1.0861	573.2	17.357
356.09	4.92	1.0843	561.8	17.486
356.09	4.84	1.0800	533.3	17.750
356.09	4.75	1.0751	501.3	19.190
356.09	4.66	1.0705	470.6	20.523
356.09	4.59	1.0665	444.7	22.513
356.09	4.49	1.0620	415.0	27.015
356.09	4.37	1.0574	384.4	30.242
356.09	4.24	1.0527	353.1	37.937
356.09	4.10	1.0476	319.2	43.864
356.09	3.98	1.0426	286.2	52.826
356.09	3.80	1.0381	256.1	60.550

T (K)	P (MPa)	n	ρ (kg · m ⁻³)	$a \cdot 10^9$ (m ² · s ⁻¹)
356.09	3.54	1.0331	222.7	75.330
356.09	3.03	1.0251	169.0	110.657
356.09	2.55	1.0187	126.1	158.419

Table VII (continued). Experimental results for R125 / isotherm $t = +1e^{-1}$

T (K)	P (MPa)	n	ρ (kg · m ⁻³)	$a \cdot 10^9$ (m ² · s ⁻¹)
373.05	8.75	1.1241	820.1	31.944
373.05	8.28	1.1196	790.5	29.968
373.05	7.90	1.1151	761.6	28.214
373.05	7.59	1.1115	738.3	27.535
373.05	7.55	1.1102	730.2	27.191
373.05	7.26	1.1059	702.1	26.861
373.05	6.98	1.1010	670.6	26.696
373.05	6.78	1.0964	640.6	26.512
373.05	6.73	1.0959	637.2	26.304
373.05	6.48	1.0904	601.6	26.502
373.05	6.30	1.0859	572.2	26.786
373.05	6.11	1.0811	540.3	27.450
373.05	5.99	1.0782	521.6	28.048
373.05	5.86	1.0746	497.9	28.971
373.05	5.65	1.0690	460.9	31.925
373.05	5.43	1.0637	425.9	35.304
373.05	5.39	1.0623	417.1	36.655
373.05	5.15	1.0571	382.7	43.372
373.05	4.86	1.0510	341.9	50.138
373.05	4.79	1.0489	327.9	52.937
373.05	4.56	1.0454	304.8	60.242
373.05	4.22	1.0398	267.3	70.332
373.05	3.93	1.0355	238.8	80.784
373.05	3.74	1.0329	221.1	85.879

Table VIII (continued). Experimental results for R143a / critical isochore

T (K)	P (MPa)	n	ρ (kg · m ⁻³)	$a \cdot 10^9$ (m ² · s ⁻¹)
345.91	3.75	1.0895	436.0	0.143
345.93	3.75	1.0895	436.0	0.189
345.96	3.75	1.0895	436.0	0.251
346.00	3.76	1.0895	436.0	0.339
346.06	3.76	1.0895	436.0	0.455
346.14	3.77	1.0895	436.0	0.617
346.26	3.78	1.0895	436.0	0.840
346.45	3.79	1.0895	436.0	1.158
346.71	3.82	1.0895	436.0	1.587
347.11	3.85	1.0895	436.0	2.180
347.68	3.90	1.0895	436.0	3.071
348.53	3.96	1.0895	436.0	4.292
349.77	4.06	1.0895	436.0	6.046

T (K)	P (MPa)	n	ρ (kg · m ⁻³)	$a \cdot 10^9$ (m ² · s ⁻¹)
351.60	4.21	1.0895	436.0	8.478
354.28	4.42	1.0895	436.0	11.739
358.21	4.74	1.0895	436.0	15.835
363.99	5.22	1.0895	436.0	21.916
372.47	5.92	1.0895	436.0	30.137

Table VIII (continued). Experimental results for R143a / 2 phase region

T (K)	P (MPa)	n_l	n_v	ρ_l (kg · m ⁻³)	ρ_v (kg · m ⁻³)	$a_l \cdot 10^9$ (m ² · s ⁻¹)	$a_v \cdot 10^9$ (m ² · s ⁻¹)
316.72	1.99	1.1786	1.0215	852.6	106.1	36.054	116.777
325.98	2.45	1.1663	1.0285	796.5	140.3	32.608	88.782
332.28	2.82	1.1557	1.0349	747.5	171.8	28.155	64.174
336.58	3.09	1.1469	1.0410	706.4	201.6	23.646	45.806
339.51	3.28	1.1395	1.0466	672.0	229.0	19.008	31.461
341.50	3.42	1.1331	1.0515	642.3	252.6	15.129	21.161
342.90	3.52	1.1261	1.0544	609.2	266.5	12.179	13.909
343.51	3.56	1.1226	1.0563	593.1	276.1	10.073	10.966
343.83	3.58	1.1211	1.0582	585.7	285.1	9.099	9.508
344.46	3.63	1.1171	1.0619	567.0	302.9	6.632	7.015
344.89	3.67	1.1135	1.0648	549.8	317.3	4.909	5.022
345.08	3.68	1.1118	1.0669	542.1	327.3	3.963	4.213
345.19	3.70	1.1104	1.0676	535.3	330.9	3.574	3.744
345.32	3.70	1.1088	1.0691	527.6	338.0	2.875	3.251
345.39	3.70	1.1082	1.0703	525.1	343.9	2.541	2.757
345.52	3.72	1.1060	1.0717	514.3	350.3	1.828	2.107
345.59	3.72	1.1049	1.0735	509.3	359.2	1.49	1.701
345.62	3.73	1.1039	1.0740	504.3	361.3	1.354	1.546
345.66	3.73	1.1033	1.0757	501.5	369.7	1.087	1.221
345.71	3.73	1.1020	1.0763	495.5	372.8	0.921	1.021
345.73	3.73	1.1012	1.0772	491.7	376.8	0.768	0.871
345.76	3.73	1.1007	1.0785	489.5	382.9	0.67	0.750
345.77	3.74	1.1002	1.0790	486.7	385.5	0.594	0.677
345.78	3.74	1.0996	1.0794	483.9	387.3	0.537	0.620

Table VIII (continued). Experimental results for R143a / isotherm $t = -5e^{-2}$

T (K)	P (MPa)	n	ρ (kg · m ⁻³)	$a \cdot 10^9$ (m ² · s ⁻¹)
328.58	8.83	1.1875	893.7	44.978
328.58	7.44	1.1837	876.5	42.233
328.58	4.87	1.1755	838.8	39.740
328.58	3.70	1.1700	813.8	36.936
328.58	2.70	1.1636	784.3	32.073
328.58	2.59	1.1625	779.2	31.231
328.58	2.59	1.0308	151.7	80.256
328.58	2.56	1.0295	145.4	85.525
328.58	2.35	1.0243	119.8	115.603
328.58	2.28	1.0235	115.9	120.153
328.58	2.00	1.0191	94.2	156.050

Table VIII (continued). Experimental results for R143a / isotherm $t = -1e^{-2}$

T (K)	P (MPa)	n	ρ (kg · m ⁻³)	$a \cdot 10^9$ (m ² · s ⁻¹)
342.42	6.87	1.1672	800.3	39.165
342.42	5.77	1.1612	773.0	36.355
342.42	5.57	1.1599	767.0	35.407
342.42	4.90	1.1549	743.6	32.747
342.42	4.57	1.1514	727.8	30.566
342.42	4.49	1.1511	726.0	30.066
342.42	4.20	1.1476	709.6	28.039
342.42	4.14	1.1465	704.8	26.556
342.42	4.02	1.1451	698.4	25.489
342.42	3.90	1.1430	688.8	23.333
342.42	3.81	1.1411	679.5	21.710
342.42	3.75	1.1398	673.6	20.951
342.42	3.69	1.1387	668.4	19.517
342.42	3.66	1.1361	656.4	17.476
342.42	3.61	1.1346	649.2	16.466
342.42	3.52	1.1313	633.9	14.798
342.42	3.50	1.1302	628.5	13.935
342.42	3.48	1.1296	625.8	13.661
342.42	3.48	1.1285	620.8	12.925
342.42	3.48	1.0545	267.0	14.817
342.42	3.48	1.0536	262.9	16.066
342.42	3.47	1.0514	252.1	20.410
342.42	3.45	1.0510	250.3	21.564
342.42	3.42	1.0482	236.6	29.473
342.42	3.37	1.0456	224.2	36.773
342.42	3.27	1.0405	199.1	50.215
342.42	3.25	1.0380	187.1	58.200
342.42	3.14	1.0362	178.0	65.173

Table VIII (continued). Experimental results for R143a / isotherm $t = -1e^{-3}$

T (K)	P (MPa)	n	ρ (kg · m ⁻³)	$a \cdot 10^9$ (m ² · s ⁻¹)
345.53	8.75	1.1710	818.1	41.585
345.53	7.92	1.1676	802.4	40.922
345.53	7.14	1.1642	786.5	38.328
345.53	6.47	1.1610	771.9	36.861
345.53	5.72	1.1562	749.6	34.465
345.53	4.88	1.1486	714.7	29.078
345.53	4.32	1.1411	679.6	23.655
345.53	4.19	1.1384	666.9	21.825
345.53	4.10	1.1362	656.5	20.484
345.53	3.99	1.1332	642.5	18.304
345.53	3.91	1.1303	629.1	16.639
345.53	3.84	1.1271	614.3	14.223
345.53	3.79	1.1230	594.7	11.157
345.53	3.76	1.1204	582.5	9.431
345.53	3.74	1.1168	565.6	6.986
345.53	3.73	1.1157	560.3	6.263
345.53	3.73	1.1106	536.4	3.912
345.53	3.73	1.1069	518.6	2.164
345.53	3.73	1.0744	363.3	1.544
345.53	3.71	1.0664	324.7	6.564
345.53	3.71	1.0649	317.8	7.782
345.53	3.70	1.0638	312.4	8.907
345.53	3.70	1.0628	307.3	9.950
345.53	3.69	1.0610	298.8	11.730
345.53	3.67	1.0586	287.3	14.872
345.53	3.65	1.0563	275.9	18.907
345.53	3.62	1.0535	262.5	24.265
345.53	3.59	1.0510	250.2	29.746
345.53	3.48	1.0445	218.6	49.277

Table VIII (continued). Experimental results for R143a / isotherm $t = +1e^{-3}$

T (K)	P (MPa)	n	ρ (kg · m ⁻³)	$a \cdot 10^9$ (m ² · s ⁻¹)
346.22	8.08	1.1683	805.6	43.174
346.22	6.09	1.1577	756.7	38.243
346.22	5.48	1.1521	730.8	34.432
346.22	4.62	1.1442	694.2	29.088
346.22	4.52	1.1423	685.3	28.154
346.22	4.39	1.1405	677.0	26.762
346.22	4.30	1.1385	667.6	24.963
346.22	4.20	1.1363	657.0	23.196
346.22	4.06	1.1324	638.8	19.803
346.22	3.95	1.1281	618.5	16.912
346.22	3.89	1.1239	598.9	13.379
346.22	3.85	1.1211	585.8	11.262
346.22	3.82	1.1163	563.4	7.931
346.22	3.81	1.1144	554.4	6.682

T (K)	P (MPa)	n	ρ (kg · m ⁻³)	$a \cdot 10^9$ (m ² · s ⁻¹)
346.22	3.80	1.1114	540.1	5.250
346.22	3.79	1.1098	532.6	4.329
346.22	3.79	1.1077	522.6	3.531
346.22	3.79	1.1057	512.8	2.782
346.22	3.79	1.1044	507.1	2.263
346.22	3.78	1.1020	495.3	1.727
346.22	3.78	1.1002	487.0	1.451
346.22	3.78	1.0988	480.4	1.236
346.22	3.78	1.0977	474.9	1.119
346.22	3.78	1.0973	473.1	1.070
346.22	3.78	1.0960	466.8	0.925
346.22	3.78	1.0933	454.2	0.776
346.22	3.78	1.0905	440.8	0.723
346.22	3.78	1.0876	426.6	0.815
346.22	3.78	1.0860	419.3	0.882
346.22	3.78	1.0839	409.1	1.088
346.22	3.77	1.0822	400.8	1.298
346.22	3.77	1.0774	377.6	2.342
346.22	3.77	1.0746	364.6	3.299
346.22	3.77	1.0724	353.9	4.422
346.22	3.76	1.0699	341.9	5.598
346.22	3.75	1.0684	334.5	6.883
346.22	3.74	1.0662	324.0	9.066
346.22	3.72	1.0625	305.8	12.718
346.22	3.71	1.0593	290.6	16.249
346.22	3.53	1.0466	229.0	41.148
346.22	3.48	1.0441	216.9	49.831

Table VIII (continued). Experimental results for R143a / isotherm $t = +1e^{-2}$

T (K)	P (MPa)	n	ρ (kg · m ⁻³)	$a \cdot 10^9$ (m ² · s ⁻¹)
349.33	8.39	1.1644	787.6	44.775
349.33	7.00	1.1571	754.2	40.379
349.33	6.24	1.1515	728.3	37.818
349.33	5.66	1.1468	706.3	35.088
349.33	5.49	1.1458	701.6	34.258
349.33	4.84	1.1385	667.5	28.492
349.33	4.78	1.1381	665.6	27.884
349.33	4.57	1.1336	644.4	24.153
349.33	4.38	1.1279	617.9	21.158
349.33	4.29	1.1245	601.8	18.676
349.33	4.25	1.1227	593.6	16.737
349.33	4.21	1.1197	579.2	14.966
349.33	4.18	1.1181	571.5	13.963
349.33	4.18	1.1156	560.0	12.057
349.33	4.17	1.1144	554.3	11.240
349.33	4.12	1.1122	543.8	10.316
349.33	4.10	1.1092	529.8	9.015

T (K)	P (MPa)	n	ρ (kg · m ⁻³)	$a \cdot 10^9$ (m ² · s ⁻¹)
349.33	4.08	1.1067	517.8	8.003
349.33	4.06	1.1025	497.7	6.836
349.33	4.05	1.1001	486.6	5.971
349.33	4.04	1.0956	465.0	5.575
349.33	4.03	1.0916	445.8	5.295
349.33	4.01	1.0881	429.3	5.345
349.33	4.00	1.0840	409.5	5.764
349.33	3.99	1.0798	389.5	6.574
349.33	3.97	1.0734	358.6	8.815
349.33	3.95	1.0696	340.5	10.838
349.33	3.92	1.0644	315.4	14.179
349.33	3.91	1.0597	292.6	18.882
349.33	3.86	1.0554	271.5	24.877
349.33	3.77	1.0493	242.1	37.222
349.33	3.65	1.0438	215.3	48.837
349.33	3.58	1.0410	201.6	56.299

Table VIII (continued). Experimental results for R143a / isotherm $t = +5e^{-2}$

T (K)	P (MPa)	n	ρ (kg · m ⁻³)	$a \cdot 10^9$ (m ² · s ⁻¹)
363.17	8.26	1.1480	711.6	39.198
363.17	7.32	1.1400	674.3	35.443
363.17	6.73	1.1336	644.8	32.016
363.17	6.33	1.1281	618.6	29.779
363.17	5.92	1.1198	579.6	25.893
363.17	5.73	1.1152	557.9	24.249
363.17	5.62	1.1120	542.9	22.839
363.17	5.50	1.1069	518.7	20.906
363.17	5.37	1.1018	494.3	19.953
363.17	5.20	1.0932	453.5	19.245
363.17	5.11	1.0885	431.0	19.139
363.17	5.01	1.0823	401.3	20.624
363.17	4.80	1.0696	340.4	27.417
363.17	4.70	1.0648	317.1	31.153
363.17	4.58	1.0600	293.8	37.110
363.17	4.38	1.0523	256.7	45.657
363.17	4.05	1.0434	213.3	61.525

Table VIII (continued). Experimental results for R143a / isotherm $t = +1e^{-1}$

T (K)	P (MPa)	n	ρ (kg · m ⁻³)	$a \cdot 10^9$ (m ² · s ⁻¹)
380.46	7.38	1.1074	521.2	32.787
380.46	7.08	1.1016	493.6	30.797
380.46	6.94	1.0987	479.5	30.390
380.46	6.81	1.0954	464.2	30.325
380.46	6.71	1.0933	453.8	30.485
380.46	6.59	1.0902	439.4	30.721
380.46	6.46	1.0870	423.7	31.442
380.46	6.30	1.0825	402.4	32.503
380.46	5.94	1.0730	356.8	37.683
380.46	5.64	1.0661	323.6	42.561
380.46	5.42	1.0596	292.0	49.145
380.46	5.19	1.0546	267.6	54.177
380.46	4.97	1.0499	244.9	62.176
380.46	4.61	1.0434	213.1	73.342